JOURNAL OF AGRICULTURAL AND FOOD CHEMISTRY

Article

Novel Trans-Ferulic Acid Derivatives Containing a Chalcone Moiety as Potential Activator for Plant Resistance Induction

Xiuhai Gan, De-Yu Hu, Yanjiao Wang, Lu Yu, and Bao-An Song

J. Agric. Food Chem., **Just Accepted Manuscript** • DOI: 10.1021/acs.jafc.7b00958 • Publication Date (Web): 03 Apr 2017

Novel *Trans*-Ferulic Acid Derivatives Containing a Chalcone Moiety as Potential Activator for Plant Resistance Induction

Xiuhai Gan,[†‡] Deyu Hu,[†] Yanjiao Wang,[†] Lu Yu,[†] Baoan Song*[†]

CORRESPONDING AUTHOR FOOT NOTE

* To whom correspondence should be addressed. Tel.: +86-851-83620521. Fax: +86-851-83622211. E-mail: songbaoan22@yahoo.com

Current address:

[†]State Key Laboratory Breeding Base of Green Pesticide and Agricultural Bioengineering, Key Laboratory of Green Pesticide and Agricultural Bioengineering, Ministry of Education, Center for Research and Development of Fine Chemicals, Guizhou University, Guiyang 550025, PR China

[‡]College of Chemistry and Life Science, Guizhou Education University, Guiyang 550018, PR China

ABSTRACT: A series of novel *trans*-ferulic acid derivatives containing a chalcone moiety were designed, and synthesized to induce plant resistance. Antiviral activities of the compounds were evaluated. Bioassay results demonstrated that compounds **F3**, **F6**, **F17**, and **F27** showed remarkable curative, protective and inactivating activities against tobacco mosaic virus (TMV). With an 50% effective concentration (EC_{50}) value of 98.78 μg mL^{-1}, compound **F27** exhibited the best protective activity compared with *trans*-ferulic acid (328.6 μg mL^{-1}), dufulin (385.6 μg mL^{-1}), and ningnanmycin (241.3 μg mL^{-1}). This protective ability was associated with potentiation of defense-related enzyme activity and activation of photosynthesis of tobacco at an early stage. This notion was confirmed by up-regulated expression of stress responses and photosynthesis regulating proteins. This work revealed that **F27** can induce resistance and enhance plant tolerance to TMV infection. Hence, **F27** can be considered as a novel activator for inducing plant resistance.

KEYWORDS: *trans-ferulic acid, chalcone, tobacco mosaic virus, antiviral activity, plant resistance*

INTRODUCTION

Tobacco mosaic virus (TMV) is a well-studied plant virus worldwide and causes massive crop loss; this virus infects more than 400 plant species of 36 families, including tobacco, tomato, potato, pepper, and cucumber.[1] Viral infection is extremely difficult to control under field conditions. Ningnanmycin (Figure 1) is the most effective plant virus inhibitor and is used to prevent TMV disease, however, this antiviral is not widely used in field trial because of the agent's photosensitivity and water stickiness.[2] In fact, no chemical treatment can thus far absolutely inhibit TMV once it has infected a plant.[3] Thus, experts face the challenge of fully protecting plants from TMV infection.

In plants, resistance induced by plant activators can provide defense against pathogens. Such resistance manifests as various defensive responses, such as oxidative burst, cell-wall reinforcement, and phytoalexin synthesis.[4–6] Some studies reported about plant activators, including salicylic acid (SA) and its derivatives,[7–9] benzo[*d*][1,2,3]-thiadiazole-7-carboxylic acid (CGA210007) and its derivatives,[6,10] and jasmonic acid (JA)[11] (Figure 1). These activators are metabolic products during plant growth. Plant metabolic products are highly efficient and environment-friendly and involve unique modes of action.[12,13] As such, these metabolic products are considered rich source of plant activators that help protect plants from TMV infection. Some metabolic products exhibit good inhibitory activities against TMV, these metabolic products include β-carbolines,[14,15] quassinoids,[16] limonoids,[17] phenanthroindolizidine and its analogues.[18] However, only few products were applied in field trials because these compounds difficult to be obtained from plants and are too complex to be synthesized.[19] Our previous research showed that the aminophosphonate derivative, dufulin (DFL) (Figure 1), displays good inhibitory activity against TMV, cucumber mosaic virus, and

other plant viruses. This derivative can activate SA signaling pathway to induce host plants to generate antiviral responses.[20] This property was widely exploited in China to prevent the spread of plant viral diseases. We also discovered a number of *α,β*-unsaturated carbonyl derivatives that exhibit good antiviral activities.[21–24] *Trans*-ferulic acid is an important *α,β*-unsaturated carbonyl metabolic product of plant (Figure 1); it is derived from cinnamic acid and can produce phytoalexins and SA through biosynthesis for defense against pathogens.[25] Some *trans*-ferulic acid derivatives were reported as anti-TMV agents.[26–28] Aside from *trans*-ferulic acid, chalcones also exhibit anti-TMV[29,30] activities. However, these compounds present low antiviral activities, and no study can explain their mechanism of action for plant resistance induction.

To further develop highly effective, full-scale antiviral agents, a series of novel *trans*-ferulic acid derivatives containing a chalcone moiety (Figure 2 and Scheme 1) were designed and synthesized to induce plant resistance in tobacco. Then, half-leaf method *in vivo*[31] was used to evaluate inhibitory activities of these agents against TMV. The present work investigated plant defense response mechanisms of compound **F27**; such mechanisms include enzyme activities, chlorophyll content, photosynthesis, and differentially expressed proteins (DEPs). To the best of our knowledge, this study first demonstrated that compound **F27** can enhance resistance in tobacco and can be considered as novel activator for plant resistance induction.

MATERIALS AND METHODS

Instruments and Chemicals. Melting points were determined on an XT-4 binocular microscope melting point apparatus (Beijing Tech Instrument Co., China; uncorrected). Nuclear magnetic resonance (NMR) spectroscopy was performed on solvents $CDCl_3$ and

dimethyl sulfoxide-d_6 (DMSO-d_6) at 500 and 125 MHz using a JEOL-ECX 500 NMR spectrometer (JEOL Ltd., Japan) and tetramethylsilane as internal standard. High-resolution mass spectrometer (HRMS) was conducted using a Thermo Scientific Q Exactive (Thermo, USA). *Trans*-ferulic acid (99% purity; CAS: 537-98-4) and other reagents were purchased from Aladdin Company. All solvents were of analytical reagent grade and were dried and purified in accordance with standard procedures before use.

General Procedures for Preparing Intermediates. *Trans*-ferulic acid ester intermediates **1a**–**1d** were synthesized with *trans*-ferulic acid and various alcohols (Scheme 1). Then, potassium carbonate (12.0 mmol) was added to a solution of corresponding intermediate **1a**–**1d** (10 mmol) in butanone (30.0 mL), and resulting mixture stirred for 1 h at room temperature. Next, 1,2-dibromoethane (15.0 mmol) was added to the mixture, which was then warmed to 80 °C and stirred for 2–4 h. Upon reaction completion (as indicated by thin-layer chromatography (TLC)), solids were removed by filtration, and solvent was removed under reduced pressure. Residue was purified by silica-gel column chromatography using petroleum ether/ethyl acetate (4:1, *v*:*v*) to obtain intermediates **2a**–**2d**. Intermediate **3** was synthesized with 4-hydroxyacetophenone and various aromatic aldehydes in accordance with reported procedures.[30]

General Synthetic Procedures for Title Compounds F1–F26. Reaction mixture was added to a solution of intermediate **3** (2.0 mmol) and potassium carbonate (2.4 mmol) in dimethylformamide (DMF) (5.0 mL), and stirred at room temperature for 1 h. A solution of corresponding intermediate **2** (1.9 mmol) in DMF (5.0 mL) was added to the mixture, which was warmed to 60 °C afterward. Stirring was continued for 2 h to 4 h. Upon

completion of reaction (indicated by TLC), cold saturated salt solution was dropwise added. Solids were filtered and washed with cold water. Crude product was recrystallized from CH_2Cl_2/CH_3OH (1:1, *v:v*) to yield 72.2% to 93.3% of title compounds **F1**–**F26**.

General Synthetic Procedures for Title Compounds F27–F30. Reaction mixture was added to a solution of corresponding acrylate (1.0 mmol) and sodium hydroxide (2.0 mmol) in H_2O (10.0 mL) and stirred at 60 °C until completion of reaction (indicated by TLC). Mixture was then acidified by dropwise addition of aqueous HCl, filtered, and then washed with cold water. Crude product was recrystallized from CH_3OH to obtain acrylic acid compounds **F27**–**F30**.

General Synthetic Procedures for Title Compounds F31–F35. Reaction mixture was added to a solution of corresponding acrylic acid (0.5 mmol) and potassium carbonate (1.0 mmol) in CH_3CN (10.0 mL) and stirred at room temperature for 0.5 h, Corresponding substituent benzyl chloride intermediate (0.5 mmol) was added to the mixture, which was then warmed to 80 °C and stirred until completion of reaction. Then, resultant mixture was filtered. Solvent was removed under reduced pressure, and crude product was recrystallized from CH_2Cl_2/CH_3OH (1:1, *v:v*) to obtain the compounds **F31**–**F35**. Section on Supporting Information list physical, NMR, and HRMS data of title compounds.

Antiviral Biological Assay. *Nicotiana. tabacum* cv. K326 and *Nicotiana. tabacum* L. plants were cultivated in a greenhouse. *N. tabacum* cv. K326 was used to determine systemic TMV infection and *N. tabacum* L. was used as local lesion host when plants grew to 5−6 leaf stage. TMV was purified by Gooding method,[32] and *in vivo* modes of compounds were determined through a reported technique; *in vivo* modes include

curative, protective, and inactivating activities.[31] Positive controls included *trans*-ferulic acid, commercial antiviral agent ribavirin, DFL, and ningnanmycin. Measurements were performed in triplicates.

Physiological and Biochemical Analysis. *Plant growth and compound treatments.* Similarly grown *N. tabacum* cv. K326 were selected at the seventh leaf stage, and 500 μg·mL^{-1} **F27** solution was smeared on whole leaves. Solvent and DFL were used as negative (CK) and positive controls, respectively. Plant leaves were inoculated with the virus after 12 h and cultivated in a greenhouse. Four treatments were adopted: CK, CK+TMV, DFL+TMV, and **F27**+TMV. Tissue samples were collected at 1, 3, 5, and 7 days after inoculation treatment for assays on chlorophyll content, photosynthetic characteristics, and defensive enzyme activities assay. Measurements were performed in triplicates.

Chlorophyll Content. Using a modified reported method,[33] Chlorophyll contents of samples were measured every two days. Test samples in triplicates of each treatment were sliced into small uniform pieces by a hole puncher while avoiding the midrib, Samples weighed 50 mg and were placed in 5 mL cold solution of 1:1 mixture of 85% acetone and 85% ethanol (*v*/*v*). Samples were homogenized, incubated for 0.5 h at 35 °C and centrifuged for 15 min at 6500 rpm. Absorbance spectra were recorded at 663 and 645 nm for chlorophyll a (C_a) and chlorophyll b (C_b), respectively, against a solution as reference. C_a, C_b, and total chlorophyll content (C_t) were calculated as follows:

$$C_a\,(mg\,L^{-1}) = 9.784OD_{663} - 0.990OD_{645}$$

$$C_b\,(mg\,L^{-1}) = 21.426OD_{645} - 4.650OD_{663}$$

$$C_t\,(mg\,L^{-1}) = C_a + C_b = 5.134OD_{663} + 20.643OD_{645}$$

Quantification (mg g^{-1} fresh weight) was performed using the following equation:

$$Q= CV/1000W$$

where C is concentration (mg L^{-1}); V is volume of solvent (mL); W refers to sample fresh weight (g).

Measurement of Photosynthetic Characteristics. With slight modifications of a described method,[34] photosynthetic characteristics of fully expanded leaves were recorded using infrared gas analyzer (Li–6400, Li–COR, Lincoln, NE, USA); these characteristics included net photosynthetic rate (P_n), stomatal conductance (G_s), intercellular CO_2 concentration (C_i), transpiration rate (T_r), and chlorophyll fluorescence (F_v/F_m) of plants treated with **F27**. Recording was conducted between 9:00 and 11:00 a.m. every two days for six plants covered by each treatment. During measurements, photosynthetic active radiation, temperature, and CO_2 concentration were 300 μmol m^{-2} s^{-1}, 30 °C, and 400 μmol mol^{-1}, respectively. Chlorophyll fluorescence was measured after adaptation to dark for 30 min to ensure complete relaxation of all reaction centers. Minimum chlorophyll fluorescence (F_0) was determined by a measuring beam, whereas maximum chlorophyll fluorescence (F_m) was measured after 0.8 s of saturation with light pulse (6000 μmol m^{-2} s^{-1}). Actinic light (300 μmol m^{-2} s^{-1}) was applied for 1 min to drive photosynthesis. Maximum quantum yield of photosystem II (PSII) (F_v/F_m) was calculated as $(F_m-F_0)/F_m$.

Determination of Defensive Enzyme Activities. Activities of superoxide dismutase (SOD), peroxidase (POD), catalase (CAT), and phenylalanine ammonia lyase (PAL) were measured and calculated with enzyme assay reagent kits in accordance with manufacturer's instructions (Suzhou Comin Bioengineering Institute, China).

DEP Analysis. *Protein Extraction.* Total tobacco proteins were extracted in accordance with reported methods with slight modifications.[35,36] Leaf sample (1.0 g) was ground to power in liquid nitrogen, homogenized, and suspended in 5 mL of ice-cold extraction buffer (0.7 M sucrose, 0.5 M Tris-HCl, 0.1 M KCl, 50 mM ethylene diamine tetraacetic acid, 40 mM dithiothreitol (DTT), pH 7.5) at room temperature for 10 min. An equal volume of phenol saturated with Tris-HCl pH 7.5 was added. Mixture was shaken at 4 °C for 30 min. After centrifugation at 5000 rpm for 10 min, the upper phenol layer was transferred to a new tube. Five volumes of 100 mM ammonium acetate in methanol were added, and resulting mixture was stored at −20 °C for 12 h. Mixture was then centrifuged at 5000 rpm and 4 °C for 20 min. Precipitate was collected and washed thrice with ice-cold 80% acetone at −20 °C. Then, precipitate was air-dried and solubilized in 150 μL rehydration solution (8 M urea, 0.1 M Tris, 10 mM DTT, PH 8.5) at 37 °C for 1 h. Protein concentration was determined using the Bradford method. Afterward, solutions containing 100 μg protein were collected. An equal volume of 55 mM iodoacetamide was added, and mixture was incubated for 30 min at room temperature in the dark. Mixture was then centrifuged at 12000 rpm and 4 °C for 20 min with 3 kDa Millipore. Protein extract was washed six times with diluent rehydration solution and dissolved in 100 μL Milli-Q water. Then, sample was incubated with 12.5 μg trypsin (Sigma, USA) at 4 °C for 30 min and then at 37 °C for at least 12 h. Mixture was centrifuged at 12000 rpm for 20 min at 4 °C. Peptide solution was collected, air-dried and solubilized in 50 μL high-performance liquid chromatography grade H_2O containing 0.1% formic acid (FA) for liquid chromatography−tandem MS (LC−MS/MS) analysis.

LC−MS/MS Analysis. Peptides were analyzed by Nano-LC−MS/MS using a Triple Time-of-flight (TOF) 5600 mass spectrometer (Foster City, CA, USA). For each sample, 8 μL peptide solution was injected using full-loop injection, and was desalted on a ChromXP Trap column (Nano LC TRAP Column, 3 μm C18-CL, 120 Å, 350 μm×0.5 mm, Foster City, CA, USA) with equilibration of 1% acetonitrile (ACN) and 0.1% FA in water. Next, each sample was washed for 10 min at 300 nL min^{-1} flow rate. Then, each sample was eluted by reverse-phase column chromatography (Nano LC C_{18}, 3 μm C18-CL, 75 μm×15 cm, Foster City, CA, USA) using linear gradient formed by mobile phase A (5% ACN, 0.1% FA) and mobile phase B (95% ACN, 0.1% FA) over 120 min at a flow rate of 300 nL min^{-1}. Eluted peptides were directed by Triple TOF 5600 MS in data-dependent mode to automatically switch between TOF–MS and product ion acquisition using Analyst (R) Software (TF1.6). β-Galactosidase digest was used to calibrate each pair of samples by 10 min of elution and 30 min of identification.

Proteomics Data Analysis. LC-MS/MS data were analyzed and quantified using MaxQuant[37] version 1.5.2.8 by Andromeda search engine and based on tobacco proteome downloaded from UniProt. Results of MaxQuant analysis included an initial search at a precursor mass tolerance of 20 ppm, which is also used for mass recalibration.[38] The search comprised variable modifications of methionine oxidation, *N*-terminal acetylation, and cysteine carbamidomethylation. Precursor mass and fragment mass presented initial mass tolerance values of 6 and 20 ppm, respectively, in the main Andromeda search. Peptide length ranged from seven amino acids to two miscleavages, and false discovery rate was set to 0.01. Normalized protein intensity was determined using label-free quantification with minimum of two ratio counts.[38] iBAQ

algorithm was used to rank absolute abundance of DEPs within a single sample.[39] Protein tables were filtered by eliminating identifications of common contaminants and reverse database. Unpaired *t*-test of iBAQ data of two-samples was used to identify differentially accumulated proteins between treatment groups and control.

Bioinformatics and annotations. Classification of DEPs was conducted with gene ontology (GO) annotation on Kyoto Encyclopedia of Genes and Genomes (KEGG) by Uniprot software (http://www.uniprot.org/). GO items lacking corresponding annotations were first removed from protein list. Subsequently, ID of listed proteins were plotted at levels of biological process, cellular component, and molecular function.[40] DEPs (expression level > 1.5 fold) were mapped to GO database (http://www.geneontology.org/), and the number of proteins at each GO term was computed. Results that came from label-free proteomics were used as the target list. Background list was generated by downloading the GO database.

Statistical analysis. Each measurement was performed in triplicates and arranged with completely randomized design. Experimental data were analyzed using SPSS Version 16.0 (SPSS, Chicago. IL, USA). Multiple comparisons were performed among different samples with Duncan's multiple-range tests ($P < 0.05$).

RESULTS AND DISCUSSION

Chemistry. Scheme 1 displays synthetic routes of *trans*-ferulic acid derivatives containing a chalcone group. *Trans*-ferulic acid methyl, ethyl, propyl, and isopropyl esters **1a**–**1d** were synthesized to determine the effects of different esters on antiviral activity. Afterward, key intermediates **2a**–**2d** were obtained from corresponding intermediates **1a**–**1d** and reacted with potassium carbonate and 1,2-dibromoethane in

butanone with a yield of 52.5% to 63.5%. Acetone, acetonitrile, tetrahydrofuran, and DMF were each used as solvents and were investigated. Low yields were acquired from the first three solvents. By contrast, compound **2** was obtained at 50% yield in DMF, but was difficult to purify with excess amounts of the chemical. Thus, butanone was considered as suitable solvent, and ratio of reactant to solvent was optimized as 1:10. Using a similar method from our previous work,[41] title compounds **F1**–**F26** were synthesized with yield of 72.2% to 93.3%. Most plant activators are carboxylic acid and their derivatives. Hence, carboxylic acid compounds **F27**–**F30** were prepared by hydrolyzing corresponding acrylates. To explore the effect of bulky groups on antiviral activity, acrylates **F31**–**F35** containing bulky groups were synthesized with corresponding acrylic acid and substituent benzyl chloride intermediates. Compounds structures were confirmed by ^{1}H NMR, ^{13}C NMR, and HRMS; data are reported in Supporting Information. In the present study, we considered **F1** as representative example. Accordingly, the main characteristic of ^{1}H NMR spectra of title compound was presence of four low-frequency downfield doublets at δ 7.93 (d, 1H, J = 16.0 Hz), 7.68 (d, 1H, J = 15.5 Hz), 7.58 (d, 1H, J = 16.0 Hz), and 6.56 (d, 1H, J = 16.0 Hz) ppm. These results reveal the presence of four *trans* =C–H protons. Two broad singlets at 4.42 and 4.35 ppm indicate that **F1** contains two O–CH_2– protons. Two singlets at 3.77 and 3.68 ppm signify that the structure contains two –OCH_3. Typical chemical shifts near δ 187.78 and 167.52 ppm of ^{13}C NMR spectra indicate the presence of C=O. Meanwhile, shifts near δ 67.43 and 67.23 ppm confirm the presence of –OCH_2–. Typical shifts near δ 56.12 and 51.87 ppm also verify the presence of –OCH_3. Electrospray ionization–HRMS showed $[M+Na]^+$ mass to be 499.15277; this value is consistent with calculated value for

$C_{28}H_{25}O_6FNa$ $[M+Na]^+$ 499.15329.

Antiviral Activity against TMV *in Vivo*. Antiviral activities of title compounds **F1**–**F35** against TMV were tested and are reported in Table 1. Some title compounds exhibited remarkable antiviral activities against TMV at 500 μg mL^{-1}. **F3**, **F6**, **F12**, **F17**, and **F19** exhibited superior curative activities with values of 63.9%, 61.9%, 56.7%, 56.3%, and 57.2%, respectively, compared with those of *trans*-ferulic acid (41.5%), DFL (43.8%), and ningnanmycin (54.5%). **F3**, **F6**, **F12**, **F13**, **F16**, **F17**, and **F19** exhibited significantly greater protective activities against TMV with values of 64.6%, 64.4%, 68.1%, 66.8, 69.4%, 68.0%, and 66.5%, respectively, than *trans*-ferulic acid (53.5%), DFL (51.4%), and ningnanmycin (62.8%). **F3**, **F6**, **F9**, **F13**, and **F17** showed superior inactivating activities with values of 92.3%, 95.3%, 92.1%, 92.6%, and 93.6%, respectively, compared with *trans*-ferulic acid (78.6%), DFL (76.5%), and ningnanmycin (91.5%). Among these compounds, **F3** (Ar = 2-F-Ph), **F6** (Ar = 4-F-Ph), and **F17** (Ar = 4-Cl-Ph) exhibited greater curative, protective and inactivating activities than *trans*-ferulic acid, DFL, and ningnanmycin. These findings implied that electron-withdrawing groups of aromatic ring can enhance antiviral activity. Further antiviral assay of carboxylic acids containing electron-withdrawing groups of aromatic rings showed that compounds **F27**–**F30** displayed better protective activities against TMV than ningnanmycin. Notably, **F27** exhibited excellent curative, protective, and inactivating activities with values of 55.6%, 71.2%, and 92.4%, respectively, which were superior to ningnanmycin. However, **F31**–**F35** demonstrated lower antiviral activities against TMV compared with ningnanmycin. These results reveal that bulk groups are unfavorable for antiviral activity of acrylate. EC_{50} values of protective activities suggest

that compounds **F3**, **F6**, **F12**, **F13**, **F16**, **F17**, **F19**, and **F25–F30** hold remarkable protective activities against TMV. EC_{50} values ranged from 98.7 μg mL^{-1} to 224.2 μg mL^{-1}. In particular, **F27** displayed the best protective activity with EC_{50} value of 97.8 μg mL^{-1}. This value was superior to those of *trans*-ferulic acid (328.6 μg mL^{-1}), DFL (385.6 μg mL^{-1}) and ningnanmycin (241.3 μg mL^{-1}).

Results of preliminary structure-activity relationships showed that electron-withdrawing groups of aromatic rings favor antiviral activity at the same position. These findings were proven by the following activity order: **F1** (Ar = 4-F-Ph) > **F5** (Ar = 4-OCH_3-Ph), **F6** (Ar = 4-F-Ph) > **F10** (4-OCH_3-Ph) and **F12** (Ar = 4-Cl-Ph) > **F23** (Ar = 4-$(CH_3)_3$-Ph). Bulky group of aromatic rings does not favor antiviral activity. This notion was supported by the activity order, **F6** (Ar = 4-F-Ph) > **F7** (Ar = 4-Cl-Ph), **F27** (Ar = 4-F-Ph) > **F28** (Ar = 4-Cl-Ph) and **F12** (Ar = 4-Cl-Ph) > **F10** (Ar = 4-OCH_3-Ph) > **F23** (Ar = 4-$(CH_3)_3$-Ph). Introducing an aromatic heterocycle also disfavors for antiviral activity. This finding was confirmed by the following activity order: **F4** (Ar = benzene) > **F11** (Ar = thiophen) > **F15** (Ar = furan). Acrylates involving suitable steric hindrance of their groups favor antiviral activity, as shown by the following activity order: **F16** (R= *i*-Pr) > **F6** (R = Et) > **F1** (R = Me) > **F32** (R = CH_2Ph) > **F34** (R = CH_2(3-CH_3-Ph)). Results also revealed that carboxylic acid compounds hold greater protective activities against TMV than those of their corresponding acrylates. This notion explains why most plant activators contain carboxyl and indicates that *trans*-ferulic acid derivatives containing a chalcone group may serve as potential anti-TMV agents.

Physiological and Biochemical Responses of Tobacco. Plants face infection by

various aggressive pathogens over their lifetime; to protect themselves during pathogenic infections, plants evolved unique immune systems and developed various defense responses; such defense mechanisms include those involving chlorophyll content, defense enzyme activity,[42] and photosynthetic rate.[43] That is, virus-infected plants develop strong physiological and biochemical alterations.

Effect on Chlorophyll Contents. As a special and the most basic life process of green plants, photosynthesis can provide necessary plant growth and energy. Chlorophylls make up core components of chloroplasts, which play a major role in photosynthesis.[44] In our study, chlorophyll content of tobacco plant (Figure 3) decreased gradually with TMV inoculation; these chlorophylls included C_a, C_b, and C_t (Figure 3A, 3B, 3C). However, in TMV-inoculated tobacco leaves treated with **F27**, chlorophyll content increased from day 1 to day 5 and reached the highest value at day 5. Variation in trends of **F27**+TMV treatment surpassed that of DFL+TMV treatment. Chlorophyll content of **F27**-treated tobacco decreased gradually. When chlorophyll content was measured, similar variation tendencies were observed in chlorophyll a/b ratios of all treatments (Figure 3D). That is, C_a and C_b, were altered simultaneously. Hence, **F27** may increase chlorophyll content, improve photosynthesis, and thereby enhance plant host resistance to diseases.

Effect on Photosynthesis. Photosynthesis is a high-rate redox metabolic process and causes reactive oxygen species (ROS) to be released in plants.[45] This process can avoid damage to plants due to excessive oxygen. In this study, we found that TMV and compound **F27** affected photosynthetic functions at various levels. P_n and T_r significantly reduced in TMV-inoculated tobacco leaves (Figure 4 A, 4C). However, responses of P_n and T_r increased in **F27**+TMV treatment group and reached their highest values on days 5

and 3, respectively. Afterward, P_n and T_r significantly declined. P_n and T_r in **F27**+TMV treatment group increased by 33.4% and 35.1%, respectively, relative to those of CK. G_s increased gradually and then decreased after treatments (Figure 4 B). C_i decreased in **F27**+TMV treatment at day 1 to day 5 and then significantly increased afterward (Figure 4 D). F_v/F_m measurement is a frequently used parameter in studies of plant ecophysiology. No significant change in F_v/F_m was noted among treatments. Notably, F_v/F_m increased after **F27**+TMV treatment (Figure 5). Photosynthesis assay results indicate that **F27** may enhance photosynthesis.

Effect on Defensive Enzyme Activities. Induced resistance is significantly related to enhanced activities of defensive enzymes, such as SOD, POD, and PAL.[42,45] Antioxidant defense machinery protects plant cells from oxidative damage induced by ROS. Furthermore, ROS generation can reflect the state of photosynthesis.[45] Therefore, we analyzed defensive enzyme activities of **F27**-treated tobacco. SOD activity of **F27**+TMV treatment group increased at day 1 to day 3 and reached the highest value on the third day. SOD activity of **F27**+TMV treatment group was higher than that of TMV-inoculated group. Then, activity decreased at day 3 to day 7 (Figure 6 A). POD activities of CK+TMV, DFL+TMV, and **F27**+TMV treatment groups were higher than that of CK. Notably, POD activity of **F27**+TMV treatment group was visibly higher than that of CK treatment group and reached the highest value (58.7%) at day 5 (Figure 6 B). As a defense gene, POD can induce biosynthetic pathway of SA, lignin, and phytoalexins, which can activate SAR[46] and promote cell-wall reinforcement and pathogen inhibition.[47] CAT can catalyze decomposition of hydrogen peroxide to water and oxygen. This process can protect cells against oxidative damage from ROS. CAT activities increased

significantly in DFL+TMV and **F27**+TMV treatment groups and reached their maximum values at day 3 (Figure 6 C). Activities (90.4% and 78.5%, respectively) were higher than that of CK treatment. In **F27** and TMV treatment groups, PAL activity of tobacco leaves increased at day 1 to day 5, reached maximum on the fifth day, and then dropped at day 5 to day 7 (Figure 6 D). PAL activity of **F27**+TMV treatment group was higher (80.0%) than that of CK group on the fifth day. PAL is a catalytic enzyme involved in biosynthesis of phenylpropanoids to cinnamic acid. Such process can produce SA for defense against pathogens.[25] Results of defensive enzyme activity assay demonstrated that **F27** can improve disease resistance of tobacco through induction defensive responses in the form of enzymes.

Identification of DEPs of Tobacco in Response to F27

In physiological and biochemical assays, the highest values of most parameters were observed on day 3. To determine the effect of proteins on TMV-inoculated tobacco after **F27** treatment, total proteins of samples on day 3 were extracted and identified through label−free LC−MS/MS. Label−free analysis revealed significant changes in proteins of treatment groups with respect to those of the control group. In total, 270 and 283 proteins were identified in CK+TMV and **F27**+TMV treatment groups, respectively (Supporting Information Table S1). A total of 244 proteins (79.0%) were common in both groups. A total of 26 and 39 proteins were unique in CK+TMV and **F27**+TMV treatment groups, respectively (Figure 7), 25 and 6 proteins were up- (**F27**+TMV versus CK+TMV ratio > 1.5, $P < 0.05$) and down-regulation (**F27**+TMV versus CK+TMV ratio < 0.7, $P < 0.05$), respectively (Supporting Information Table S2).

Functional classification by GO

To assign functional information to DEPs between TMV plants and those treated with **F27**+TMV, GO analysis was carried out; this analysis can provide hierarchical relationships for representation of information on cellular components, molecular function, and biological processes.[48] As shown in Figure 8, Go term enrichment analysis of DEPs ($P < 0.05$) showed that main cellular components involved "membrane", "membrane part", "thylakoid", "plastid thylakoid", "plastid thylakoid membrane", "chloroplast thylakoid", "chloroplast thylakoid membrane", "chloroplast envelope", "photosystem", "photosystem II", and "photosynthetic membrane". Molecular function included "cation binding", "metal-ion binding", "ion binding", "calcium-ion binding", and "electron carrier activity". Main biological process were "electron transport chain", "cation transport", "regulation of defense response", "regulation of response to stress", "response to toxin", and "regulation of response to stimulus". Protein ratio of regulating immune response accounted for 22.6% of total DEPs, including heat shock protein 26, constitutive plastid-lipid-associated protein, SOD (Cu-Zn), putative glutathione S-transferase, and dehydroascorbate reductase. Results of GO analysis indicated that compound **F27** can strongly reshape tobacco proteome by influencing many aspects of plant physiology; some of these aspects include stress responses and photosynthesis.

Functional classification by KEGG

To further investigate the relationship between DEPs and biological functions, KEGG was used to identify potential biological pathways of DEPs between CK+TMV and **F27**+TMV treatment groups. DEPs were mapped to KEGG database categories at $P < 0.05$. Only two pathways were enriched: photosynthesis (pathway ID, ko00195) and amyotrophic lateral sclerosis (pathway ID, ko00195). Enriched pathways included 10 and

2 DEPs, respectively. These results revealed that photosynthesis is a significant pathway for DEPs, as shown in Table 2 and Figure 9. Photosynthesis regulated by seven up- and three down-regulated expressed proteins, respectively.

Identification of proteins related to photoreaction system

Photosynthesis is one of the most important metabolic processes in plants; it requires four protein components of photosynthetic electron transport chain, which is responsible for electron transfer from water to oxidized form of nicotinamide adenine dinucleotide phosphate, including PSII, PSI, cytochrome complex, and adenosine triphosphate synthase. As shown in Figure 9 and Table 2, 10 DEPs were observed in **F27**+TMV versus CK+TMV treatment groups. These DEPs included ETR12 (2.28-fold), PsbP2 (2.10-fold), PsbQ (2.07-fold), PsbP3 (1.64-fold), PetC2 (1.59-fold), PsbO (1.54-fold), and PsaEB (1.51-fold); they were distinctly up-regulated in **F27**+TMV than in CK+TMV treatment group. However, only three down-regulated proteins were found in **F27**+TMV versus CK+TMV treatment groups; this down-regulation caused changes in structure and function of the four protein components in photosynthetic organism pathway. As extrinsic proteins, PsbO, PsbP, and PsbQ are subunits of oxygen-evolving complex, which is a core of PSII in high plants. These extrinsic proteins are located at luminal surface of PSII and are attached to its intrinsic subunits.[49] PsbO protein is termed as manganese-stabilizing protein and is involved in regulation of PSII affinity for Mn. PsbO protein is also required for PSII assembly/stability in higher plants and protects CP43 and CP47 from proteolytic attack.[50] PsbP and PsbQ are involved in increasing binding affinities for both calcium and chloride, which are essential cofactors for oxygen evolution.[51] Results indicated that compound **F27** increased expression quantity of

protein-regulated photoreaction system. **F27** also activated immunity system and enhanced plant tolerance to TMV infection.

In summary, 35 novel *trans*-ferulic acid derivatives containing a chalcone moiety were designed and synthesized to induce plant resistance. Results showed that compounds **F3**, **F6**, **F17**, and **F27** exhibited better curative, protective and inactivating activities than those of ningnanmycin. Especially, compound **F27** exhibited the best protective activity among title compounds. This protective ability was associated with potentiation of defensive enzyme activity, chlorophyll content, and photosynthesis of tobacco after treatment with **F27**. This finding was confirmed by up-regulated expression of stress responses and photosynthesis regulatory proteins. This study demonstrated that **F27** can induce resistance and enhance plant tolerance to TMV infection. **F27** can also be considered as novel potential activator in field of plant protection.

ASSOCIATED CONTENT

Supporting Information

Supporting information illustrates synthesis, characterizations, physical, and analytical data of intermediate **2a**–**2d** and **3**, target compounds **F1**–**F35**, and DEPs of **F27**+TMV versus CK+TMV. This material is available free of charge via the Internet at http:// pubs.acs.org.

AUTHOR INFORMATION

Corresponding Author

*Tel.: +86-851-83620521. Fax: +86-851-83622211. E-mail: songbaoan22@yahoo.com.

ACKNOWLEDGMENTS

We gratefully acknowledge the assistance from the National Natural Science Foundation

of China (21362004).

Notes

The authors declare no competing financial interest.

REFERENCES

(1) Craeger, A. N.; Scholthof, K. B.; Citovsky, V.; Scholthof, H. B. Tobacco mosaic virus: pioneering research for a century. *Plant cell* **1999**, *11*, 301–308.

(2) Chen, M. H.; Chen, Z.; Song, B. A.; Bhadury, P. S.; Yang, S.; Cai, X. J.; Hu, D. Y.; Xue, W.; Zeng, S. Synthesis and antiviral activities of chiral thiourea derivatives containing an R-aminophosphonatemoiety. *J. Agric. Food Chem.* **2009**, *57*, 1383–1388.

(3) Reichman, M.; Devash, Y.; Suhadolnik, R. J.; Sela, I. Human leukocyte interferon and the antiviral factor (AVF) from virus-infected plants stimulate plant tissues to produce nucleotides with antiviral activity. *Virology* **1983**, *128*, 240–244.

(4) Kim, Y.; Komoda, E.; Miyashita, M.; Miyagawa, H. Continuous stimulation of the plant immune system by the peptide elicitor PIP1 is required for phytoalexin biosynthesis in tobacco cells. *J. Agric. Food Chem.* **2014**, *62*, 5781−5788.

(5) Jones, J. D.; Dangl, J. L. The plant immune system. *Nature* **2006**, *444*, 323–329.

(6) Du, Q. S.; Zhu, W. P.; Zhao, Z. J.; Qian, X. H.; Xu, Y. F. Novel benzo-1,2,3-thiadiazole-7-carboxylate derivatives as plant activators and the development of their agricultural applications. *J. Agric. Food Chem.* **2012**, *60*, 346−353.

(7) Silverman, F. P.; Petracek, P. D.; Ju, Z.; Fledderman, C. M.; Heiman, D. F.; Warrior, P. Salicylate activity. 1. Protection of plants from paraquat injury. *J. Agric. Food Chem.* **2005**, *53*, 9764–9768.

(8) Silverman, F. P.; Petracek, P. D.; Ju, Z.; Fledderman, C. M.; Heiman, D. F.; Warrior, P.

Salicylate activity. 2. Potentiation of atrazine. *J. Agric. Food Chem.* **2005**, *53*, 9769–9774.

(9) Silverman, F. P.; Petracek, P. D.; Heiman, D. F.; Fledderman, C. M.; Warrior, P. Salicylate activity. 3. Structure relationship to systemic acquired resistance. *J. Agric. Food Chem.* **2005**, *53*, 9775–9780.

(10) Fan, Z. J.; Shi, Z. G.; Zhang, H. K.; Liu, X. F.; Bao, L. L.; Ma, L.; Zuo, X.; Zheng, Q. X.; Mi, N. Synthesis and biological activity evaluation of 1,2,3-thiadiazole derivatives as potential elicitors with highly systemic acquired resistance. *J. Agric. Food Chem.* **2009**, *57*, 4279–4286.

(11) Kauss, H.; Krause, K.; Jeblick, W. Methyl jasmonate conditions parsley suspension cells for increased elicitation of phenylpropanoid defense responses. *Biochem. Biophys. Res. Commun.* **1992**, *189*, 304–308.

(12) Qian, X. H.; Lee, P. W.; Cao, S. China: forward to the green pesticides via a basic research program. *J. Agric. Food Chem.* **2010**, *58*, 2613–2623.

(13) Seiber, J. N. Sustainability and agricultural and food chemistry. *J. Agric. Food Chem.* **2011**, *59*, 1–21.

(14) Chen, J.; Yan, X. H.; Dong, J. H.; Sang, P.; Fang, X.; Di, Y. T.; Zhang, Z. K.; Hao, X. J. Tobacco mosaic virus (TMV) inhibitors from *Picrasma quassioides* Benn. *J. Agric. Food Chem.* **2009**, *57*, 6590−6595.

(15) Song, H. J.; Liu, Y. X.; Liu, Y. X.; Wang, L. Z.; Wang, Q. M. Synthesis and antiviral and fungicidal activity evaluation of *β*-carboline, dihydro-*β*-carboline, tetrahydro-*β*-carboline alkaloids, and their derivatives. *J. Agric. Food Chem.* **2014**, *62*, 1010–1018.

(16) Yan, X. H.; Chen, J.; Di, Y. T.; Fang, X.; Dong, J. H.; Sang, P.; Wang, Y. H.; He, H. P.; Zhang, Z. K.; Hao, X. J. Anti-tobacco mosaic virus (TMV) quassinoids from *Brucea javanica* (L.) Merr. *J. Agric. Food Chem.* **2010**, *58*, 1572−1577.

(17) Ge, Y. H.; Liu, K. X.; Zhang, J. X.; Mu, S. Z.; Hao, X. J. The limonoids and their antitobacco mosaic virus (TMV) activities from *Munronia unifoliolata* Oliv. *J. Agric. Food Chem.* **2012**, *60*, 4289−4295.

(18) Wang, Z. W.; Wei, P.; Wang, L. Z.; Wang, Q. M. Design, synthesis, and anti-tobacco mosaic virus (TMV) activity of phenanthroindolizidines and their analogues. *J. Agric. Food Chem.* **2012**, *60*, 10212–10219.

(19) Isman, M. B. Botanical insecticides: For richer, for poorer. *Pest Manage. Sci*. **2008**, *64*, 8−11.

(20) Chen, Z.; Zeng, M. J.; Song, B. A.; Hou, C. R.; Hu, D. Y.; Li, X. Y.; Wang, Z. C.; Fan, H. T.; Bi, L.; Liu, J. J.; Yu, D. D.; Jin, L. H.; Yang, S. Dufulin activates HrBP1 to produce antiviral responses in tobacco. *PLoS one* **2012**, *7*, e37944.

(21) Luo, H.; Liu, J. J.; Jin, L. H.; Hu, D. Y.; Chen, Z.; Yang, S.; Wu, J.; Song, B. A. Synthesis and antiviral bioactivity of novel (1*E*,4*E*)-1-aryl-5-(2-(quinazolin-4-yloxy)phenyl)-1,4-pentadien-3-one derivatives. *Eur. J. Med. Chem.* **2013**, 6*3*, 662–669.

(22) Ma, J.; Li, P.; Li, X. Y.; Shi, Q. C.; Wan, Z. H.; Hu, D.Y.; Jin, L. H.; Song, B. A. Synthesis and antiviral bioactivity of novel 3-((2-((1*E*,4*E*)-3-oxo-5-arylpenta-1,4-dien-1-yl)phenoxy)methyl)-4(3*H*)-quinazolinone derivatives. *J. Agric. Food Chem.* **2014**, *62*, 8928–8934.

(23) Han, Y.; Ding, Y.; Xie, D. D.; Hu, D. Y.; Li, P.; Li, X. Y.; Xue, W.; Jin, L. H.; Song, B. A. Design, synthesis and antiviral activity of novel rutin derivatives containing

1,4-pentadien-3-one moiety. *Eur. J. Med. Chem.* **2015**, *92*, 732–737.

(24) Long, C. W.; Li, P.; Chen, M. H; Dong, L. R.; Hu, D. Y.; Song, B. A. Synthesis, anti-tobacco mosaic virus and cucumber mosaic virus activity, and 3D-QSAR study of novel 1,4-pentadien-3-one derivatives containing 4-thioquinazoline moiety. *Eur. J. Med. Chem.* **2015**, *102*, 639–647.

(25) Gozzo, F. Systemic acquired resistance in crop protection: from nature to a chemical approach. *J. Agric. Food Chem.* **2003**, *51*, 4487–4503.

(26) Ouyang, M. A.; Wein, Y. S.; Zhang, Z. K.; Kuo, Y. H. Inhibitory activity against tobacco mosaic virus (TMV) replication of pinoresinol and syringaresinol lignans and their glycosides from the root of *Rhus javanica* var. *roxburghiana*. *J. Agric. Food Chem.* **2007**, *55*, 6460–6465.

(27) Wu, M.; Wang, Z. W.; Meng, C. S.; Wang, K. L.; Hu, Y. N.; Wang, L. Z.; Wang, Q. M. Discovery and SARs of *trans*-3-aryl acrylic acids and their analogs as novel anti-tobacco mosaic virus (TMV) agents. *PLoS one*. **2013**, *8*, e56475.

(28) Huang, G. Y.; Cui, C.; Wang, Z. P.; Li, Y. Q.; Xiong, L. X.; Wang, L. Z.; Yu, S. J.; Li, Z. M.; Zhao, W. G. Synthesis and characteristics of (Hydrogenated) ferulic acid derivatives as potential antiviral agents with insecticidal activity. *Chem. Cent. J.* **2013**, *7*, 33–44.

(29) Du, G.; Han, J. M.; Kong, W. S.; Zhao, W.; Yang, H. Y.; Yang, G. Y. Chalcones from the flowers of *rosa rugosa* and their anti-tobacco mosaic virus activities. *B. Kor. Chem. Soc.* **2013**, *34*, 1263–1265.

(30) Wan, Z. H.; Hu, D. Y.; Li, P.; Xie, D. D.; Gan, X. H. Synthesis, antiviral bioactivity of novel 4-thioquinazolinederivatives containing chalcone moiety. *Molecules* **2015**, *20*,

11861–11874.

(31) Song, B. A.; Zhang, H. P.; Wang, H.; Yang, S.; Jin, L. H.; Hu, D. Y.; Pang, L. L.; Xue, W. Synthesis and antiviral activity of novel chiral cyanoacrylate derivatives. *J. Agric. Food. Chem*. **2005**, *53*, 7886–7891.

(32) Gooding, G. V. Jr.; Hebert, T. T. A simple technique for purification of tobacco mosaic virus in large quantities. *Phytopathology* **1967**, *57*, 1285–1287.

(33) Zhao, J.; Zhou, J. J.; Wang, Y. Y.; Gu, J. W.; Xie, X. Z. Positive regulation of phytochrome B on chlorophyll biosynthesis and chloroplast development in rice. *Rice Science* **2013**. *20*, 243–248.

(34) Yi, X. P.; Zhang, Y. L.; Yao, H. S.; Luo, H. H.; Gou, L.; Chow, W. S.; Zhang, W. F. Different strategies of acclimation of photosynthesis, electron transport and antioxidative activity in leaves of two cotton species to water deficit. *Functional Plant Biology* **2016**, *43*, 448–460.

(35) Tahara, S. T.; Mehta, A.; Rosato, Y. B. Proteins induced by *Xanthomonas axonopodis* pv. *passiflorae* with leaf extract of the host plant (*Passiflorae edulis*). *Proteomics* **2003**, *3*, 95–102.

(36) Qian, G. L.; Zhou, Y. J.; Zhao, Y. C.; Song, Z. W.; Wang, S. Y.; Fan, J. Q.; Hu, B. S.; Venturi, V.; Liu, F. Q. Proteomic analysis reveals novel extracellular virulence-associated proteins and functions regulated by the diffusible signal factor (DSF) in *Xanthomonas oryzae* pv. *oryzicola*. *J. Proteome Res.* **2013**, *12*, 3327−3341.

(37) Cox, J.; Neuhauser, N.; Michalski, A.; Scheltema, R. A.; Olsen, J. V.; Mann, M. Andromeda: a peptide search engine integrated into the MaxQuant environment. *J Proteome Res.* **2011**, *10*, 1794–1805.

(38) Cox, J.; Michalski, A.; Mann, M. Software lock mass by two-dimensional minimization of peptide mass errors. *J. Am. Soc. Mass Spectr.* **2011**, *22*, 1373–1380.

(39) Luber, C. A.; Cox, J.; Lauterbach, H.; Fancke, B.; Selbach, M.; Tschopp, J.; Akira, S.; Wiegand, M.; Hochrein, H.; O'Keeffe, M.; Mann, M. Quantitative proteomics reveals subset-specific viral recognition in dendritic cells. *Immunity* **2010**, *32*, 279–289.

(40) Gene Ontology Consortium. The gene ontology (GO) database and informatics resource. *Nucleic. Acids Res.* **2004**, *32*, 258–261.

(41) Gan, X. H.; Hu, D. Y.; Li, P.; Wu, J.; Chen, X. W.; Xue, W.; Song, B. A. Design, synthesis, antiviral activity and three-dimensional quantitative structure-activity relationship study of novel 1,4-pentadien-3-one derivatives containing the 1,3,4-oxadiazole moiety. *Pest Manag. Sci.* **2016**, *72*, 534–543.

(42) Fan, H. T.; Song, B. A.; Bhadury, P. S.; Jin, L. H.; Hu, D. Y.; Yang, S. Antiviral activity and mechanism of action of novel thiourea containing chiral phosphonate on tobacco mosaic virus. *Int. J. Mol. Sci.* **2011**, *12*, 4522–4535.

(43) Rahoutei, J.; García-Luque, I.; Barón, M. Inhibition of photosynthesis by viral infection: effect on PSII structure and function. *Physiol. Plant.* **2000**, *110*, 286–292.

(44) Ahmad, I.; Cheng, Z. H.; Meng, H. W.; Liu, T. J.; Nan, W. C.; Khan, M. A.; Wasila, H.; Khan, A. R. Effect of intercropped garlic (*Allium sativum*) on chlorophyll contents, photosynthesis and antioxidant enzymes in pepper. *Pak. J. Bot.* **2013**, *45*, 1889–1896.

(45) Dietz, K. J.; Turkan, I.; Krieger-Liszkay, A. Redox- and reactive oxygen species-dependent signaling into and out of the photosynthesizing chloroplast. *Plant Physiol*. **2016**, *171*, 1541–1550.

(46) Nyström, L.; Mäkinen, M.; Lampi, A. M.; Piironen, V. Antioxidant activity of steryl

ferulate extract from rye and wheat bran. *J. Agric. Food Chem.* **2005**, *53*, 2503–2510.

(47) Nicholson, R. L.; Hammerschmidt, R. Phenolic compounds and their role in disease resistance. *Annu. Rev. Phytopathol.* **1992**, *30*, 369−389.

(48) Ashburner, M.; Ball, C. A.; Blake, J. A.; Botstein, D.; Butler, H.; Cherry, J. M; Davis, A. P.; Dolinski, K.; Dwight, S. S.; Eppig, J. T.; Harris, M. A.; Hill, D. P.; Issel-Tarver, L.; Kasarskis, A.; Lewis, S.; Matese, J. C.; Richardson, J. E.; Ringwald, M.; Rubin, G. M.; Sherlock, G. Gene ontology: tool for the unification of biology. *Nat. Genet.* **2000**, *25*, 25–29.

(49) Chen, L. B.; Jia, H. Y.; Du, L. B.; Tian, Q.; Gao, Y. L.; Liu, Y. Release of the oxygen-evolving complex subunits from photosystem II membranes in phosphorylation condition under light stress. *Chin. J. Chem.* **2011**, *29*, 2631–2636.

(50) Popelkova, H.; Commet, A.; Kuntzleman, T.; Yocum, C. F. Inorganic cofactor stabilization and retention: the unique functions of the two PsbO subunits of eukaryotic photosystem II. *Biochemistry* **2008**, *47*, 12593–12600.

(51) Mummadisetti, M. P.; Frankel, L. K.; Bellamy, H. D.; Sallans, L.; Goettertb, J. S.; Brylinski, M.; Limbachc, P. A.; Bricker, T. M. Use of protein cross-linking and radiolytic footprinting to elucidate PsbP and PsbQ interactions within higher plant Photosystem II. *Proc. Natl. Acad. Sci. U.S.A.* **2014**, *111*, 16178–16183.

Table, Scheme and Figure Captions

Table 1. *In Vivo* Antiviral Activities of Test Compounds against TMV

Table 2. DEPs Involved in Photoreaction Systems

Scheme 1. Synthetic Route for Title Compounds

Figure 1. Structures of some plant activators and antiviral compounds.

Figure 2. Design of title compounds.

Figure 3. Effects of compound **F27** on C_a (A), C_b (B), C_t (C), and Chlorophyll a/b (D) in tobacco leaves. Vertical bars refer to mean ± SD (n = 3).

Figure 4. Effects of compound **F27** on P_n (A), G_s (B), T_r (C), and C_i (D) in tobacco leaves. Vertical bars refer to mean ± SD (n = 3).

Figure 5. Effects of compound **F27** on F_v/F_m in tobacco leaves. Vertical bars refer to mean ± SD (n = 3).

Figure 6. Effects of compound **F27** on SOD (A), POD (B), CAT (C), and PAL (D) activity in tobacco leaves. Vertical bars refer to mean ± SD (n = 3).

Figure 7. Changed proteome distribution between **F27**+TMV and CK+TMV, Venn diagram showing unique and shared proteins.

Figure 8. Cellular components, molecular functions, and biological processes involving DEPs in **F27**+TMV versus CK+TMV.

Figure 9. KEGG map of photosynthetic pathway of DEPs in **F27**+TMV versus CK+TMV. Boxes with red frame indicate the corresponding DEPs were up-regulated in **F27**+TMV samples. Boxes with green frame indicate that corresponding DEPs were down-regulated in **F27**+TMV samples.

Table 1. *In Vivo* Antiviral Activities of Test Compounds against TMV[a]

Compd.	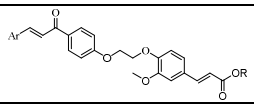		Curative activity[b] (%)	Protective activity[b] (%)	Inactivating activity[b] (%)	EC_{50} of protective activity (μg mL^{-1})
	R	Ar				
F1	Me	4-F-Ph	40.0±2.1	58.2±2.4	89.3±2.3	304.7±3.1
F2	Me	4-Cl-Ph	50.4±3.9	51.4±0.6	89.0±1.5	442.5±3.6
F3	Me	2-F-Ph	63.9±3.0	64.6±1.1	92.3±1.9	214.2±1.9
F4	Me	-Ph	52.4±2.3	61.1±1.8	88.9±3.7	281.1±1.4
F5	Me	4-OCH_3-Ph	21.5±1.8	56.4±2.0	87.5±2.3	311.4±5.1
F6	Et	4-F-Ph	61.9±3.4	64.4±3.1	95.3±1.1	217.6±2.1
F7	Et	4-Cl-Ph	43.5±4.1	49.7±3.3	61.7±2.3	487.9±3.7
F8	Et	2-F-Ph	39.8±3.5	55.9±1.9	81.4±1.9	333.3±2.8
F9	Et	-Ph	30.0±3.9	58.5±3.8	92.1±0.4	330.5±1.9
F10	Et	4-OCH_3-Ph	32.7±2.3	56.7±3.1	79.6±2.6	279.1±2.1
F11	Me	thiophen	46.6±1.9	49.8±3.6	80.7±1.4	549.1±2.5
F12	*n*-pr	4-Cl-Ph	56.7±2.7	68.1±3.5	85.8±4.5	208.3±1.6
F13	*n*-pr	2-F-Ph	31.0±2.3	66.8±6.7	92.6±1.6	210.1±2.9
F14	*n*-pr	-Ph	43.8±5.1	54.7±1.3	91.3±2.9	346.0±3.2
F15	Me	furan	43.8±2.8	45.8±2.3	84.7±2.1	534.4±3.1
F16	*i*-Pr	4-F-Ph	32.9±4.6	69.4±1.9	87.6±2.7	193.5±2.2
F17	*i*-Pr	4-Cl-Ph	56.3±1.2	68.0±2.5	93.6±1.0	162.2±1.9
F18	*i*-Pr	2-F-Ph	40.3±3.9	57.7±5.0	90.4±2.5	269.4±4.2
F19	Me	3-F-Ph	57.2±1.9	66.5±2.6	87.9±1.9	224.2±1.2
F20	Me	2,4-diF-Ph	45.6±2.1	53.7±2.7	85.8±1.7	414.4±4.0
F21	Me	2,6-diF-Ph	41.3±1.7	51.4±1.9	89.9±0.7	403.1±3.2
F22	*n*-pr	2,4-diOCH_3-Ph	33.1±3.2	56.5±2.9	89.5±2.3	369.3±1.9
F23	*n*-pr	4-$C(CH_3)_3$-Ph	18.7±2.8	54.3±3.4	78.8±1.9	405.4±4.0
F24	*i*-Pr	2,4-diCl-Ph	27.8±2.1	62.3±2.7	90.2±2.8	292.5±3.2
F25	Me	4-Br-Ph	45.2±1.5	64.3±2.5	87.2±2.9	201.5±2.2
F26	Me	2-Cl-Ph	48.5±3.1	65.7±2.4	79.2±2.2	189.6±3.5
F27	H	4-F-Ph	55.6±3.3	71.2±2.9	92.4±0.8	98.7±1.5
F28	H	4-Cl-Ph	51.2±2.6	68.5±2.8	81.7±1.6	185.4±1.2
F29	H	2-F-Ph	52.6±4.1	68.7±1.5	74.3±2.4	164.9±3.7
F30	H	2-Cl-Ph	48.5±2.2	65.7±3.1	75.8±3.5	183.4±5.1
F31	CH_2Ph	2-F-Ph	49.2±3.7	62.5±3.3	93.5±1.5	248.5±1.7
F32	CH_2Ph	4-F-Ph	51.1±3.2	60.5±1.1	90.1±0.3	265.6±3.1
F33	CH_2(2,4-diCl-Ph)	4-F-Ph	53.4±5.1	54.8±3.1	87.1±0.9	312.2±3.1
F34	CH_2(3-CH_3-Ph)	4-F-Ph	46.3±4.5	49.5±1.6	88.3±1.7	458.2±3.2
F35	CH_2(2,4-diCl-Ph)	4-Cl-Ph	52.8±2.4	60.1±0.6	89.4±0.5	298.8±2.6
trans-ferulic acid[c]			41.5±2.7	53.5±1.8	78.6±2.5	328.6±3.1
dufulin[d]			43.8±2.5	54.1±1.6	76.5±2.8	385.6±3.9
ningnanmycin[d]			54.5±2.3	62.8±1.9	91.5±2.1	241.3±1.2

[a]Average of three replicates. [b]Concentration of compounds is 500 μg·mL^{-1}. [c]Purity ≥ 99%. [d]Commercial antiviral agent ribavirin and ningnanmycin as positive control.

Table 2. DEPs Involved in Photoreaction Systems

Accession	Protein Name	F27+TMV:TMV	*p*-value	regulated
Q6RUN4	ETR12	2.28	3.07E-07	up
P18212	PsbP2	2.10	2.24E-07	up
Q53UI6	PsbQ	2.07	2.45E-08	up
Q04127	PsbP3	1.64	3.95E-07	up
Q02585	PetC2	1.59	5.65E-09	up
Q40459	PsbO	1.54	1.52E-11	up
Q41229	PsaEB	1.51	7.91E-08	up
Q40432	PsaH	0.51	9.50E-07	down
G3LV29	PsbB	0.57	9.70E-10	down
G3LUY2	atpF-b	0.61	8.02E-10	down

TOC graphic

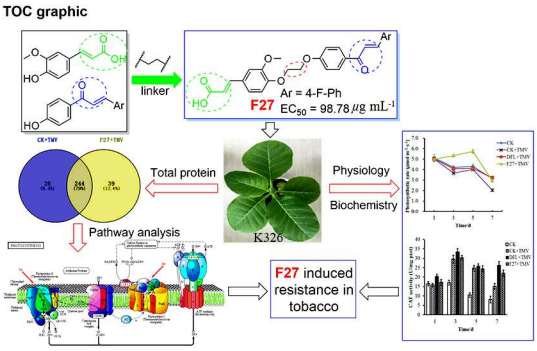
TOC graphic
linker
Ar = 4-F-Ph
F27 EC50 = 98.78 μg mL-1
Total protein
Physiology
Biochemistry
Pathway analysis
K326
F27 induced resistance in tobacco

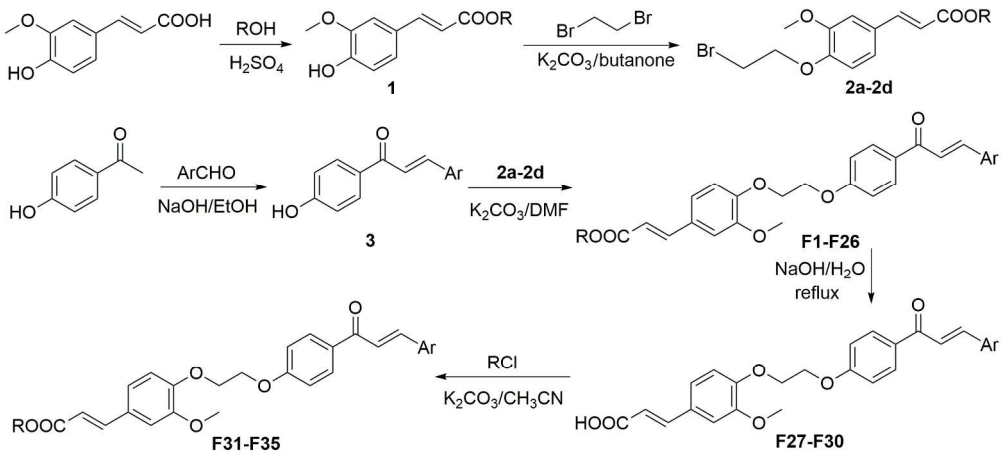

Scheme 1. Synthetic Route for Title Compounds

193x88mm (300 x 300 DPI)

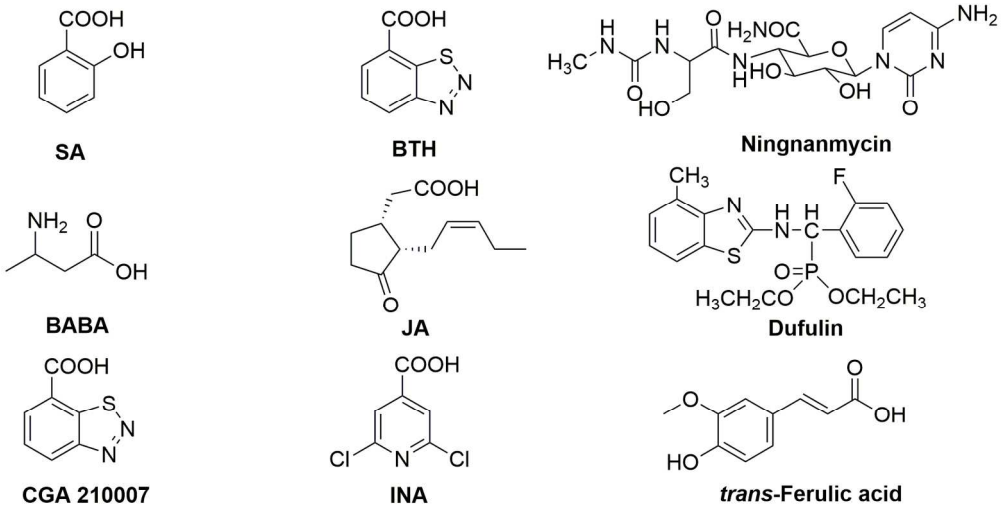

Figure 1. Structures of some plant activators and antiviral compounds.

161x83mm (300 x 300 DPI)

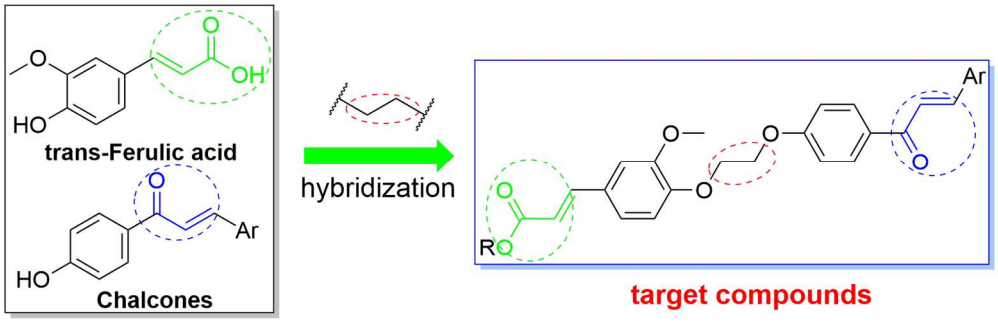

Figure 2. Design of title compounds.

152x49mm (300 x 300 DPI)

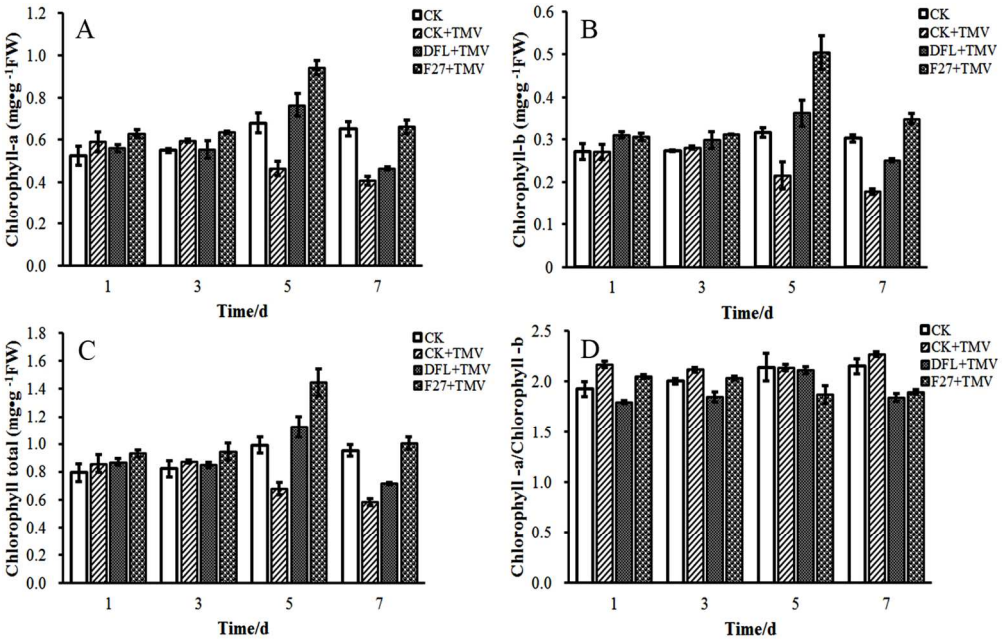

Figure 3. Effects of compound F27 on Ca (A), Cb (B), Ct (C), and Chlorophyll a/b (D) in tobacco leaves. Vertical bars refer to mean ± SD (n = 3).

130x83mm (300 x 300 DPI)

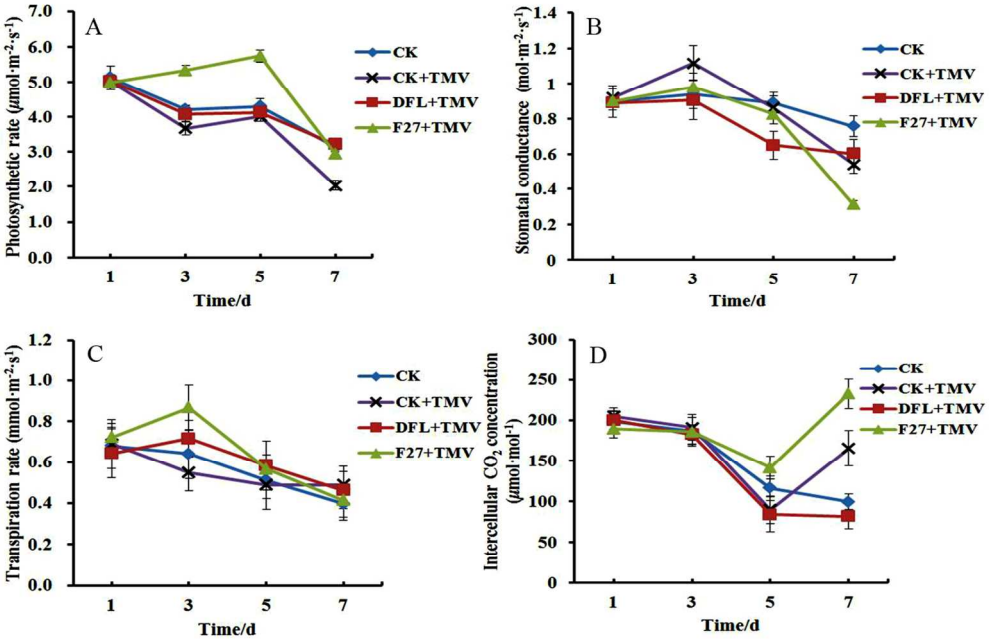

Figure 4. Effects of compound F27 on Pn (A), Gs (B), TR (C), and Ci (D) in tobacco leaves. Vertical bars refer to mean ± SD (n = 3).

124x81mm (300 x 300 DPI)

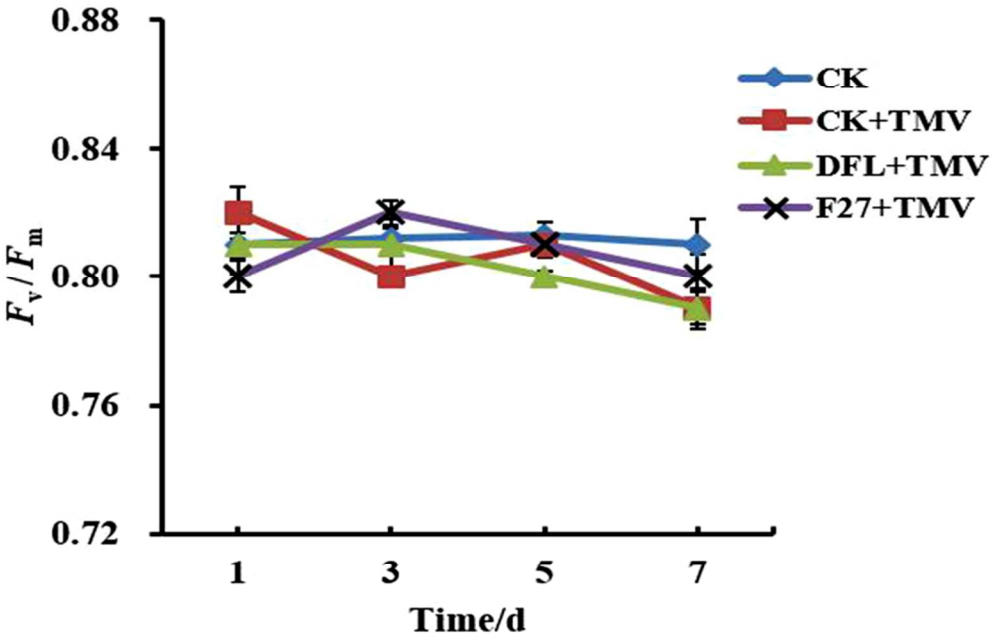

Vertical bars refer to mean ± SD (n = 3).

Figure 5. Effects of compound F27 on Fv/Fm in tobacco leaves. Vertical bars refer to mean ± SD (n = 3).

87x58mm (300 x 300 DPI)

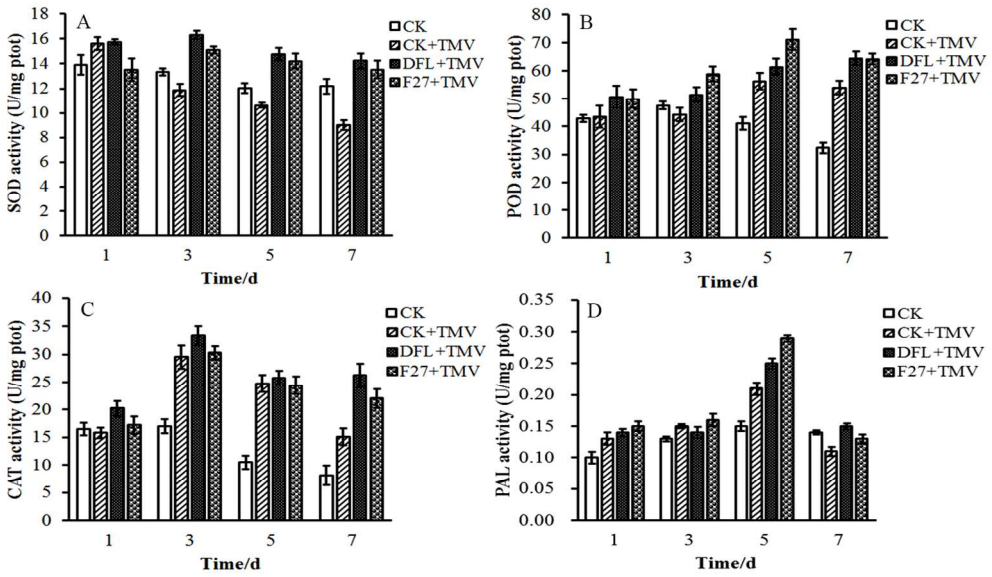

Figure 6. Effects of compound F27 on SOD (A), POD (B), CAT (C), and PAL (D) activity in tobacco leaves. Vertical bars refer to mean ± SD (n = 3).

134x76mm (300 x 300 DPI)

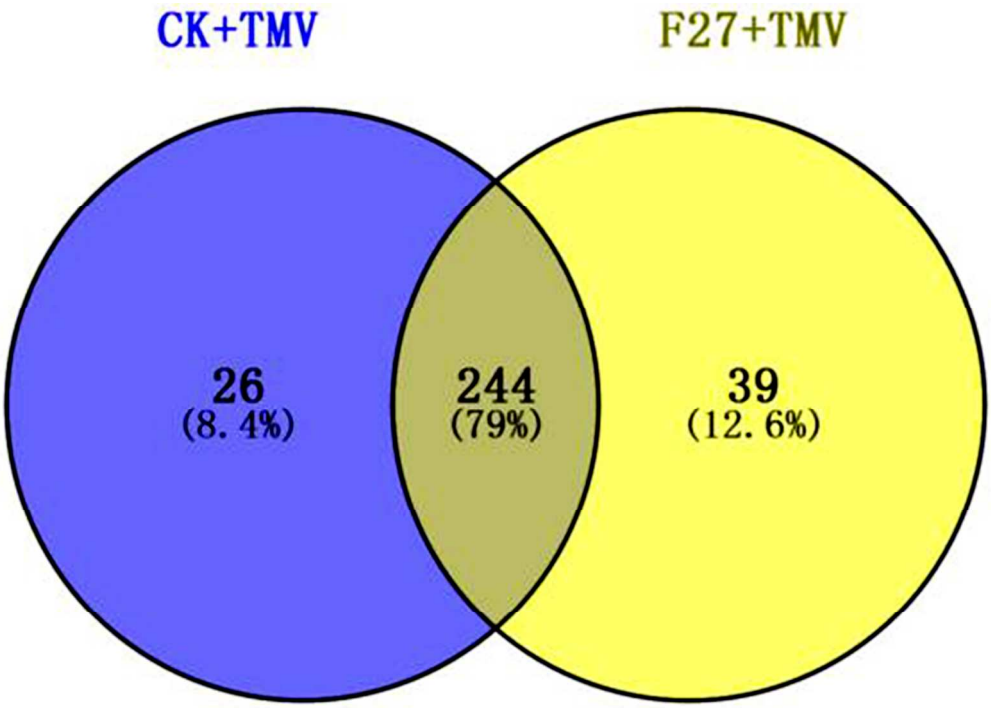

Figure 7. Changed proteome distribution between F27+TMV and CK+TMV, Venn diagram showing unique and shared proteins.

131x93mm (300 x 300 DPI)

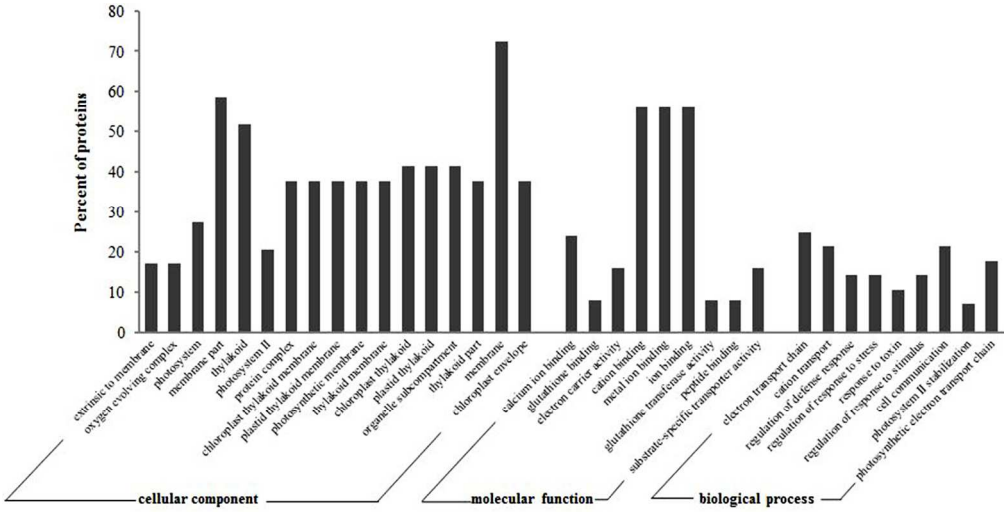

Figure 8. Cellular components, molecular functions, and biological processes involving DEPs in F27+TMV versus CK+TMV.

229x116mm (300 x 300 DPI)

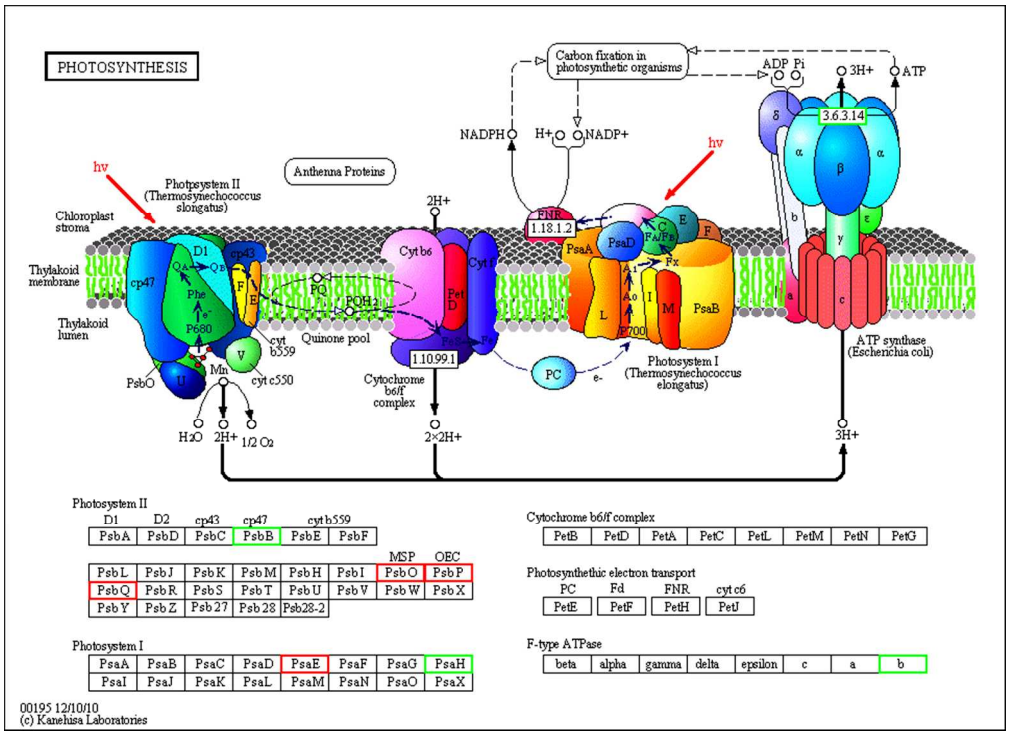

Figure 9. KEGG map of photosynthetic pathway of DEPs in F27+TMV versus CK+TMV. Boxes with red frame indicate the corresponding DEPs were up-regulated in F27+TMV samples. Boxes with green frame indicate that corresponding DEPs were down-regulated in F27+TMV samples.

339x245mm (300 x 300 DPI)

TOC graphic

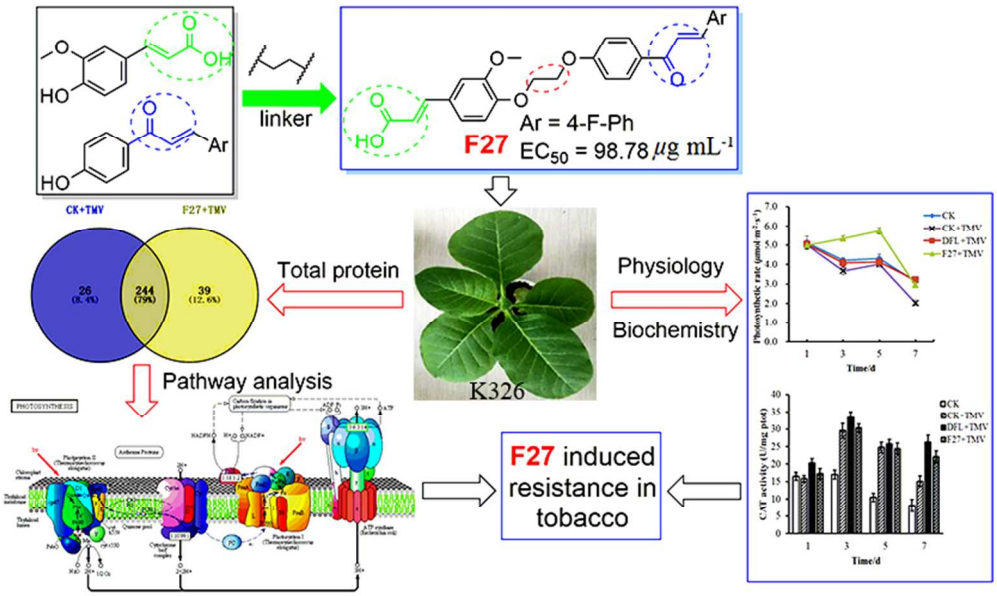

Top Graphic

70x45mm (300 x 300 DPI)

Graphical Abstract

Thirty-five novel *trans*-ferulic acid derivatives containing a chalcone moiety were designed and synthesized. Compounds **F3**, **F6**, **F17**, and **F27** exhibited remarkable anti-TMV activities and compound **F27** induced resistance in tobacco.